Beyond the G-Loop: CRBN Molecular Glues Potently Target VAV1 via a Novel SH3 RT-Loop Degron

Hanfeng Lin [a,b,c,†], Xin Yu [a,b,†], Haiyang [a,b], Ran Cheng [a,b], Xiaoli Qi [a,b], Yen-Yu Yang [d], Shengmin Zhou[e], Xing Che[e], Jin Wang [a,b,f]

[a.] The Verna and Marrs McLean Department of Biochemistry and Molecular Pharmacology, Baylor College of Medicine, Houston, Texas 77030, United States.

[b.] Center for NextGen Therapeutics, Baylor College of Medicine, Houston, Texas 77030, United States.

[c]. Graduate Program in Chemical, Physical & Structural Biology, Graduate School of Biomedical Sciences, Baylor College of Medicine, Houston, Texas 77030, United States.

[d]. Thermo Fisher Scientific, San Jose, California 95134, United States.

[e]. YDS Pharmatech, Inc., Albany, New York 12226, United States.

[f]. Department of Molecular and Cellular Biology, Baylor College of Medicine, Houston, Texas 77030, United States.

[†.] These authors contribute equally.

Corresponding email: wangj@bcm.edu

Abstract

This study reports the discovery and characterization of novel CRBN molecular glues that selectively induce the proteasomal degradation of the hematopoietic-specific signaling protein VAV1, a key target in hematological malignancies and autoimmune diseases. Utilizing unbiased global proteomics, we identified phenyl-glutarimide derivatives NGT-201-12, as effective VAV1 degraders, with its C-terminal SH3 domain ($SH3^2$) being crucial for this interaction. A significant finding is the elucidation of a non-canonical RT-loop degron (RDxS motif, residues 796-799) within VAV1 $SH3^2$, distinct from previously characterized G-loop degrons. This discovery, supported by advanced computational modeling using the YDS-GlueFold platform and validated by site-directed mutagenesis, highlights versatility of CRBN in recognizing diverse neosubstrate motifs.

Introduction

The ubiquitin-proteasome system (UPS) is a fundamental cellular machinery responsible for maintaining protein homeostasis through the selective degradation of a vast array of intracellular proteins, including those that are misfolded, damaged, or naturally short-lived [1]. This intricate process is critical for normal cellular function, and its dysregulation is implicated in numerous human diseases[1]. In recent years, the therapeutic strategy of Targeted Protein Degradation (TPD) has gained prominence, aiming to eliminate disease-causing proteins by hijacking the UPS [2–7]. Among TPD approaches, molecular glue degraders have emerged as a compelling class of small molecules [8]. These agents function by inducing or stabilizing the protein-protein interaction (PPI) between an E3 ubiquitin ligase and a specific target protein (a neosubstrate), which is then polyubiquitinated and subsequently degraded by the proteasome [9–13].

Cereblon (CRBN), a substrate receptor for the Cullin-RING E3 ubiquitin ligase 4 ($CRL4^{CRBN}$) complex, is a well-established E3 ligase that can be effectively modulated by molecular glues [8,10,14]. The therapeutic utility of CRBN modulation was first highlighted by immunomodulatory drugs (IMiDs)—thalidomide, lenalidomide, and pomalidomide [9,15,16]. These drugs bind to CRBN, allosterically altering its substrate specificity to promote the degradation of neosubstrates such as the lymphoid transcription factors IKZF1 and IKZF3, which is crucial for their anti-myeloma activity [9,11]. The profound clinical success of IMiDs has not only validated CRBN as a druggable E3 ligase but has also catalyzed extensive research efforts aimed at discovering novel CRBN modulators capable of degrading a wider array of pathogenic proteins [17–19].

The discovery of novel molecular glues, however, remains a significant challenge due to the indirect nature of their mechanism, which complicates rational design efforts [8,13]. Historically, many glues were found serendipitously [20], through target-driven screening using reporter assay system [21], or comparative phenotypic screening in E3-deficient cell models [22]. Modern approaches increasingly rely on systematic strategies, especially advanced proteomic techniques for unbiased neosubstrate identification and selectivity profiling. Degradation-based global proteomics enables direct identification of degradable neosubstrates [12]. Proximity-based proteomics helps identify transient protein-protein interaction mediated by lead compounds [23,24]. Enrichment-based chemoproteomics, for instance, allows for the mapping of proteins recruited to CRBN by specific compounds [18]. Furthermore, computational tools like YDS-GlueFold is combining diffusion model with statistic mechanics for predicting ternary complex structures and guiding molecular design [25], while FEP+ binding free energy calculation in the ternary system for explaining cooperativity and target selectivity [26].

VAV1, a hematopoietic-specific signaling protein, is a key regulator of immune cell development and function [27]. It acts as both a guanine nucleotide exchange factor (GEF) for Rho/Rac family GTPases and as an adaptor protein, playing critical roles in T-cell receptor (TCR) and B-cell receptor (BCR) signaling pathways that govern calcium mobilization, ERK activation, cytoskeletal rearrangements, and gene transcription [28]. Dysregulation of VAV1, through mutations or aberrant expression, has been linked to various hematological malignancies including T-cell lymphomas, and autoimmune diseases [29]. Given its multifaceted role in disease and its hematopoietic-specific expression, VAV1 presents an attractive therapeutic target [30]. Traditional inhibitors might only partially modulate VAV1's functions, whereas its complete elimination via targeted protein degradation could offer a more comprehensive therapeutic effect by ablating both its catalytic and scaffolding activities [28].

In this study, we report the identification and characterization of novel CRBN molecular glues that selectively target VAV1 for degradation. Utilizing an unbiased, deep global proteomics-based approach enabled by Thermo Orbitrap Astral Mass Spectrometer, we identified NGT-201-11 and NGT-201-12, an analog with enhanced potency, as effective VAV1 degraders. Mechanistic investigations employing a luminescence-based HiBiT-RR protein quantification system [31] with VAV1 truncation mutants localized the essential degron to the C-terminal SH3 domain ($SH3^2$) of VAV1. Importantly, leveraging the YDS-GlueFold platform [25], we computationally modeled the CRBN:NGT-201-12:VAV1-$SH3^2$ ternary complex, predicting critical interactions involving VAV1 R796 and the RT loop of the $SH3^2$ domain. While established structural biology techniques like CryoEM and X-ray crystallography are considered the gold standards for determining molecular structures, they typically require highly optimized compounds and conditions, especially for resolving complex assemblies [11]. In contrast, the YDS-GlueFold platform provides a significant advantage by enabling the prediction of ternary complex structures during the early stages of drug discovery—precisely when such structural information can be most impactful for guiding compound design and optimization. Site-directed mutagenesis studies functionally validated this predicted RT loop, specifically an RDxS motif (residues 796-799), as a non-canonical degron essential for NGT-201-12-mediated degradation. This finding is significant as it deviates from the canonical G-loop degrons typically recognized by CRBN [8]. Further chemical optimization (NGT-201-17, NGT-201-18), led to a marked potentiation of VAV1 degradation.

Results

Proteomics Screening Identifies VAV1 as a Neosubstrate of Novel CRBN Glue

To investigate novel avenues of CRBN-mediated protein degradation, an unbiased, quantitative mass spectrometry-based proteomics approach was utilized to screen a phenyl-glutarimide centric library [32,33], analyzing cellular proteomes after treatment with candidate CRBN-based molecular glue compounds (**Figure 1A, B**). From this library, NGT-201-11 and NGT-201-12, possessing similar substitution patterns on the core phenyl-glutarimide scaffold, were concurrently identified as compounds capable of inducing VAV1 degradation, albeit to different degrees. Cellular treatment with NGT-201-11 led to a modest yet statistically significant decrease in VAV1 protein levels compared to the vehicle controls (**Figure 1C**). NGT-201-12 demonstrated a substantially more pronounced degradation of VAV1 (**Figure 1D**). The dose-responsive degradation of VAV1 by both compounds was subsequently confirmed through Western blot analysis (**Figure 1E**). These findings validated the potential of this chemotype and highlighted NGT-201-12 as a promising candidate for more detailed mechanistic studies and further optimization.

VAV1 exhibits a modular structure comprising tandem $SH3^1$-SH2-$SH3^2$ domains on its C-terminus integral to its signaling capacity. To precisely delineate the VAV1 region mediating interaction with the CRBN:NGT-201-12 complex, a luminescence-based protein quantification approach utilizing the HiBiT-RR system was employed to avoid tag-mediated degradation artifacts [31]. A series of VAV1 truncation mutants fused to the small HiBiT-RR peptide tag was generated. Consistent with expectations, cells expressing full-length VAV1-HiBiT-RR constructs demonstrated robust, dose-dependent reduction in luminescence signal following NGT-201-12 treatment. When truncating domains from the C-terminus, we discovered that removal of the first SH3 domain on the C-terminus ($SH3^2$) is sufficient to abrogate NGT-201-12-induced VAV1 degradation (**Figure 1F**). These findings

localize the essential degron recognized by the CRBN-NGT-201-12 complex to the C-terminal SH3[2] domain of VAV1.

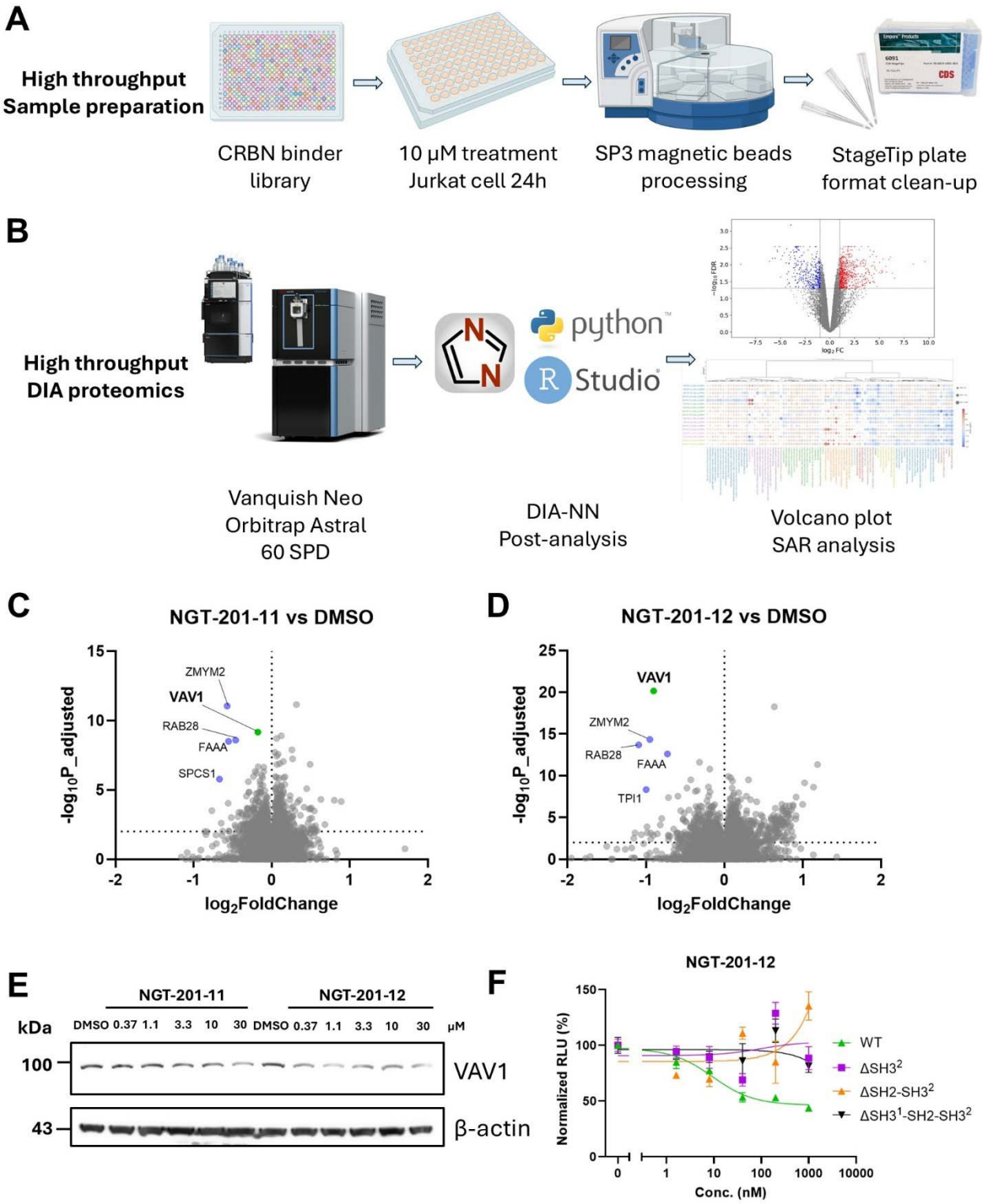

Figure 1. Proteomics Screening Identifies VAV1 as a Neosubstrate of Novel CRBN Glues and Localization of the Degron to the C-terminal SH3 Domain.

(**A**) Schematic representation of the high-throughput DIA proteomics workflow employed to identify potential CRBN neosubstrates. (**B**) Overview of the DIA-NN data processing and statistical analysis pipeline. (**C, D**) Volcano plots depicting protein abundance changes in Jurkat cells treated with 10 µM

NGT-201-11 (C) or (D) NGT-201-12 for 24 hours compared to DMSO control. VAV1 is green highlighted. Other significantly downregulated proteins are in blue. (**E**) Western blot analysis confirming the dose-dependent degradation of endogenous VAV1 by 24 hours NGT-201-11 and NGT-201-12 treatment in Jurkat cells. (**F**) HiBiT-based dose-response curves illustrating the degradation of full-length VAV1 (WT) and various truncation mutants (ΔSH3², ΔSH2-SH3², ΔSH3¹-SH2-SH3²) upon 24 hours treatment with increasing concentrations of NGT-201-12 in Hela cells. Loss of the C-terminal SH3 domain (ΔSH3²) abolishes NGT-201-12-induced degradation. Data are presented as mean ± SD from three independent experiments.

Ternary Complex Modeling Predicts Key Molecular Interactions

To obtain structural insights into the mechanism by which NGT-201-12 facilitates the association between CRBN and the VAV1 $SH3^2$ domain, we used GlueFold [25], developed by YDS Pharmatech, Inc., to predict the ternary complex structure of CRBN: NGT-201-12 :VAV1-$SH3^2$. Following extensive sampling, we identified predicted structures with the highest ipTM score between CRBN and VAV1-$SH3^2$ of 0.807.

The resultant structural model furnished valuable atomic-level hypotheses concerning the binding interface (**Figure 2A**). To functionally validate the interface predicted by the YDS-GlueFold model, the putative PPI surface on the VAV1 $SH3^2$ domain was systematically interrogated via site-directed mutagenesis. Residues situated within surface-exposed loops, particularly those predicted to mediate contact with CRBN or NGT-201-12, were mutated, primarily to alanine. The impact of these mutations on compound-induced degradation was subsequently quantified using the nano-luciferase (nLuc)-VAV1 reporter system. Evaluation of mutants treated with NGT-201-12 revealed that mutations within the RT loop exerted the most profound effects on degradation efficiency (**Figure 2B**). Specifically, alanine mutation of the core RDxS motif residues—Arg796 (R796A), Asp797 (D797A), Ser799 (S799A) or S799R (mimicking VAV2/3)—resulted in a dramatic loss of degradation potency, effectively abrogating the dose-response relationship observed with wild-type VAV1 (**Figure 2B**). Conversely, mutation of Arg798 to alanine (R798A) or methionine (R798M, mimicking VAV2/3), paradoxically enhanced degradation potency and D_{max} (**Figure 2B**). We hypothesize that the bulk guanidinium side chain of R798 may impose a suboptimal steric conformation for the VAV1 SH3² domain within the CRBN-NGT-201-12 ternary complex. Replacement with smaller or conformationally distinct residues promotes more efficient PPI and subsequent degradation. Mutations at CRBN:VAV1 interface outside the immediate RT loop, such as Q818A, exhibited more moderate effects on NGT-201-12-induced degradation, whereas mutation of Trp820 (W820A), predicted to be at the VAV1:NGT-201-12 interface, significantly reduced degradation potency (**Figure 2C**). Collectively, these functional mutagenesis data strongly implicate the RT loop, and specifically the RDxS sequence (residues 796-799), as the critical, non-canonical degron within the VAV1 $SH3^2$ domain essential for mediating the interaction with the CRBN-molecular glue complex. This finding stands in marked contrast to the canonical G-loop degrons identified in previously characterized IMiD neosubstrates and underscores the capacity of CRBN-glue complexes to recognize diverse structural motifs for neosubstrate recruitment.

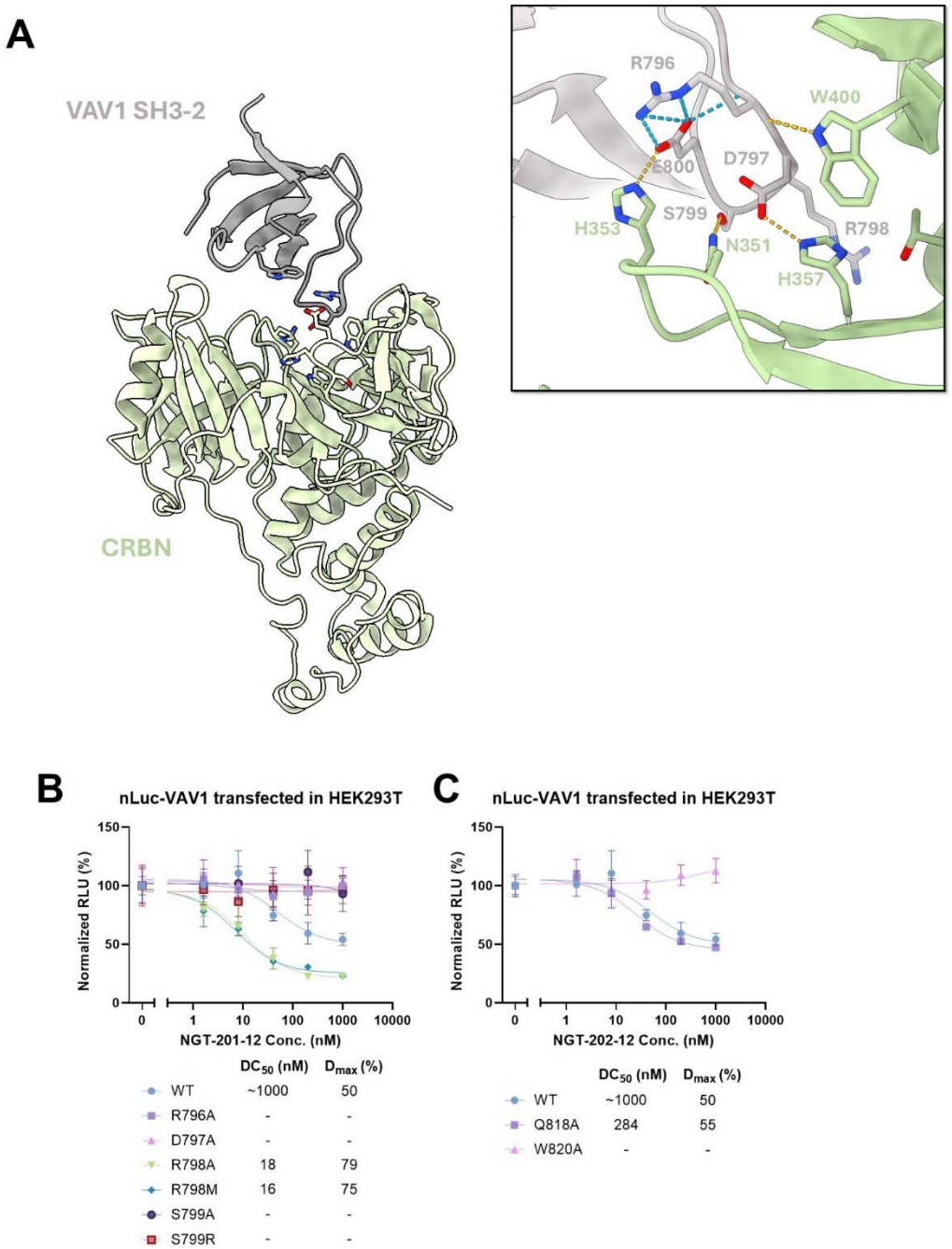

Figure 2. Ternary Complex Modeling and Mutagenesis Identify a Non-Canonical RT Loop Degron in VAV1 SH3^2.

(**A**) Computational model of the NGT-201-12-induced ternary complex formed between CRBN and the VAV1 SH3^2 domain. NGT-201-12 was not shown, CRBN in light green, and VAV1 SH3^2 in gray. Close-up view of the predicted interaction interface between NGT-201-12 and the VAV1 SH3^2 domain RT loop region, illustrating potential hydrogen bonds (cyan dashed lines) and hydrophobic interactions (yellow dashed lines). Key VAV1 SH3^2 residues within the RT loop are labeled. (**B, C**) Dose-response curves showing the effect of NGT-201-12 on the degradation of wild-type (WT) nLuc-VAV1 and various point mutants within the predicted CRBN/NGT-201-12 interaction interface in HEK293T cells. Data are presented as mean ± SD from three independent experiments. The table inset in (E) and (F) summarizes the DC_{50} and D_{max} values for each mutant.

Correlation Between FEP+ Energy Ranking and Experimental Degradation Potencies

Based on domain deletion experiments, mutation analysis and folding results, we developed and synthesized eight analogs seeking to improve the activities of NGT-201-11 and NGT-201-12. We tested these compounds using Jurkat VAV1-HiBit knock-in cell line and measured the %Dmax at 1uM and logIC50 (Table 1). To explore the potential of GlueFold folding method to rank future compounds before synthesis, we folded these compounds with VAV1 and CRBN and tested different ranking/scoring methods. We first adopted Schrodinger Glide Docking to score the folded structures. Each predicted ternary structure was prepared with Schrodinger Protein Preparation Workflow and converted into Grid, and ligands were prepared with Schrodinger LigPrep. Docking was conducted with extra precision (XP) and summarized in Table 1. Spearman correlation for ranks shows that docking scores show a weak positive correlation with Dmax at 1uM and weak negative correlation with logIC50 (Figure 3). Because a lower docking score/predicted binding free energy indicates a higher affinity, we concluded that docking method was not able to provide meaningful correlation and prediction to explain the medicinal chemistry behind our data.

Table 1. Glide docking scores, %Dmax at 1uM and logIC50 for tested candidates.

Compound Name	%Dmax @1uM	logIC50	Glide Docking Score (kcal/mol)
NGT-201-11	30.44	-6.91	-12.98
NGT-201-110	87.71	-7.87	-11.18
NGT-201-112	40.43	-5.75	-12.49
NGT-201-119	68.22	-7.85	-13.89
NGT-201-12	89.35	-7.27	-11.60
NGT-201-125	77.42	-7.13	-12.18
NGT-201-13	63.27	-6.54	-8.48
NGT-201-133	49.20	-5.87	-12.75
NGT-201-14	95.02	-8.38	-10.78
NGT-201-18	88.55	-7.46	-11.93

Recently, we noticed a computational method to rank molecular glue degraders. In their manuscript, Dudas et al. used Schrodinger FEP+ to calculate relative cooperativity for molecular glue ternary structures by the following expression[1]:

$$\Delta\Delta G^0_{\text{coop}} = \Delta\Delta G^0_{ALB} - \Delta\Delta G^0_{A,L} - \Delta\Delta G^0_{L,B}$$

We selected NGT-201-18 GlueFold prediction as the receptor for simulation. We first docked all the ligands into predicted protein with predicted NGT-201-18 structures as the reference ligand. Then, the receptor and docked ligands were used for FEP+ relative binding energy calculation. For binary energy predictions ($\Delta\Delta G^0_{A,L}$, $\Delta\Delta G^0_{L,B}$), we removed the other protein and use the structure for FEP+. When building the map for simulation, we selected NGT-201-11 and NGT-201-12 as biased nodes, for their representative structural features in our tested compounds. We summarized the simulation results in Table 2. Spearman correlation shows a positive ρ at 0.72 for $\Delta\Delta G^0_{\text{coop}}$ and logIC50 and a negative ρ at -0.77 for $\Delta\Delta G^0_{\text{coop}}$ and %Dmax, which aligns with the scientific logic and also shows a moderate prediction capability. Furthermore, if we consider NGT-201-11 and NGT-201-12 as the starting points and use -1 kcal/mol as the cutoff for selection criteria, then the four selected compounds, NGT-201-110, NGT-201-119, NGT-201-125 and NGT-201-18 all have better %Dmax than NGT-201-11 and NGT-201-12. In a practical scenario, we would be able to achieve 100% positive rate by using GlueFold and Schrodinger FEP+ workflow.

Table 2. FEP+ calculated $\Delta\Delta G^0_{coop}$, %Dmax at 1uM and logIC50 for tested candidates.

Compound Name	%Dmax @1uM	logIC50	$\Delta\Delta G^0_{coop}$ (kcal/mol)
NGT-201-11	30.44	-6.91	0.00
NGT-201-110	87.71	-7.87	-1.50
NGT-201-112	40.43	-5.75	-0.33
NGT-201-119	89.35	-7.27	-1.20
NGT-201-12	68.22	-7.85	-0.09
NGT-201-125	77.42	-7.13	-1.17
NGT-201-13	63.27	-6.54	0.06
NGT-201-133	49.20	-5.87	1.86
NGT-201-14	88.55	-7.46	-0.37
NGT-201-18	95.02	-8.38	-1.42

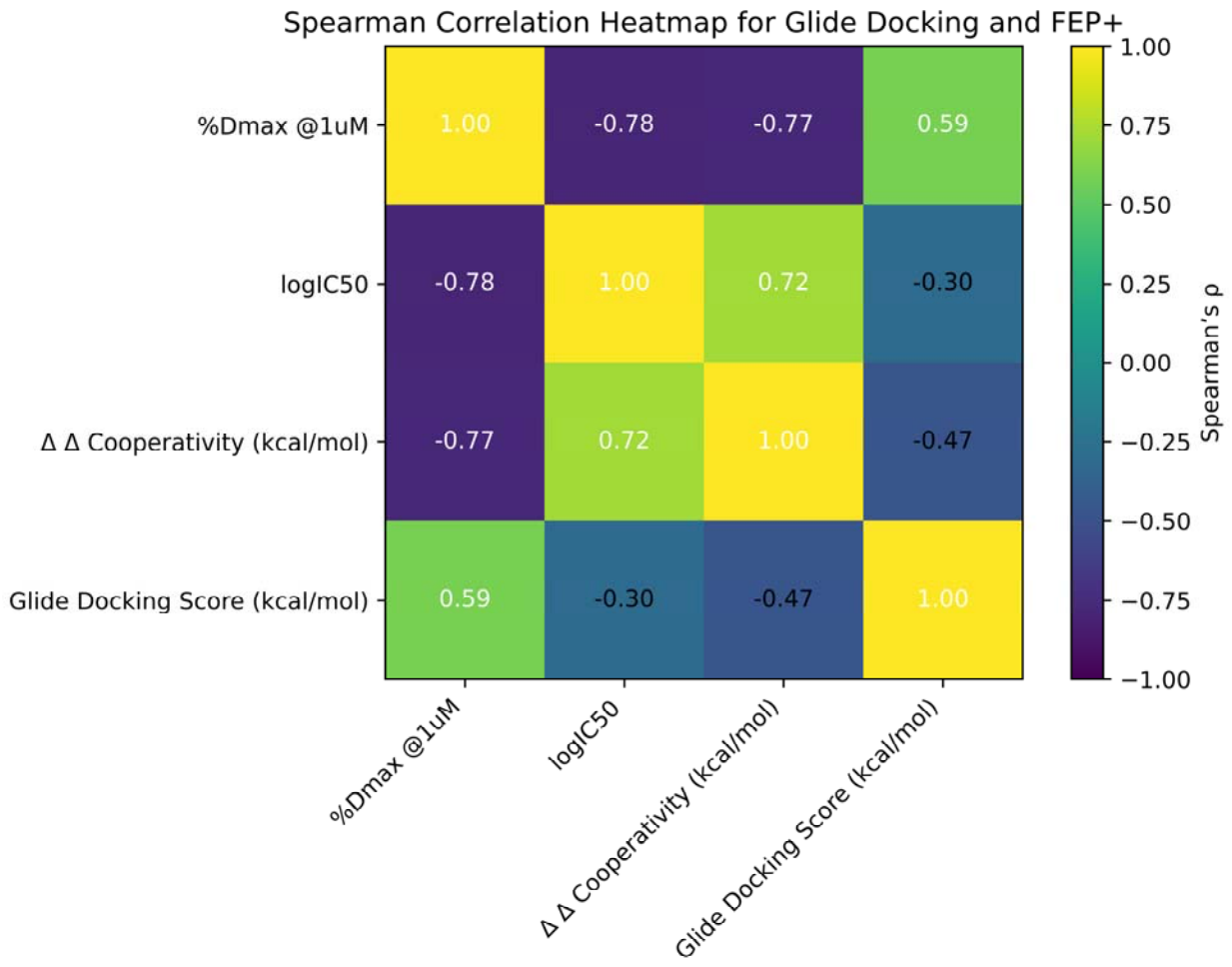

Figure 3. Spearman correlation heatmap for Glide Docking and FEP+.

Discussion

Our study successfully identified and characterized novel CRBN molecular glues that selectively target the hematopoietic-specific signaling protein VAV1 for proteasomal degradation. Utilizing an unbiased, deep global proteomics approach, we discovered that phenyl-glutarimide derivatives, notably NGT-201-12, can effectively induce VAV1 degradation. Mechanistic investigations pinpointed the C-terminal SH3 domain ($SH3^2$) of VAV1 as crucial for this process. This research significantly expands our understanding of molecular glue mechanisms and offers a promising strategy for targeting VAV1, a protein implicated in various hematological malignancies and autoimmune diseases.

A key finding of this work is the elucidation of a non-canonical degron within the VAV1 $SH3^2$ domain. While CRBN molecular glues are often associated with the recognition of G-loop degrons, our computational modeling and subsequent site-directed mutagenesis studies compellingly demonstrated that an RT loop, specifically an RDxS motif (residues 796-799), is essential for the NGT-201-12-mediated degradation of VAV1. This discovery highlights the versatility of CRBN as an E3 ligase capable of recognizing diverse structural motifs on neosubstrates, moving beyond the canonical G-loop paradigm. The identification of this novel RT-loop degron opens new avenues for

designing molecular glues against targets previously considered intractable due to the absence of known degron motifs.

This study further underscores the potent synergy between predictive structural modeling and iterative chemical optimization in the development of effective protein degraders. We leveraged the YDS-GlueFold platform, an advanced computational tool prioritizing protein-protein interactions (PPIs) with superior capabilities than AlphaFold3. This platform successfully predicted the key intermolecular contacts within the ternary complex formed by our lead compound, CRBN, and the VAV1 $SH3^2$ domain, including crucial PPIs between CRBN and VAV1. These structural hypotheses were subsequently validated experimentally through our site-directed mutagenesis studies.

While definitive techniques like Cryo-EM and X-ray crystallography remain the gold standard for high-resolution structural elucidation, their demanding requirements for highly optimized compounds and experimental conditions often mean that ternary complex structures are determined retrospectively. As a result, their direct impact on prospectively guiding the initial hit-to-lead optimization in drug discovery can be limited, with many reported structures serving as post-hoc analyses. In contrast, the YDS-GlueFold platform offers a significant strategic advantage by enabling the generation of actionable structural models of ternary complexes during the critical early phases of discovery. This timing is precisely when such structural insights are most valuable for iteratively guiding medicinal chemistry efforts. Access to these predictive ternary complex models empowers researchers to employ structure-based drug design strategies, including molecular docking and rational de novo design, to more efficiently engineer compounds with enhanced potency and desired pharmacological properties.

Competing Interest Statement

J.W. is the co-founder of Chemical Biology Probes LLC. J. W. has stock ownership in CoRegen Inc and serves as a consultant for this company. J.W. and X.Y. are the co-founders of Fortitude Biomedicines, Inc. and hold equity interest in this company. J.W., H.L. and X.Y. are the coinventors of a patent application related to the disclosed VAV1 degraders. S.Z., X.C. are YDS Pharmatech Inc. Employees.

Acknowledgement

The research was supported in part by National Institute of Health (R01-CA268518 and R01-CA250503 to J.W.), the Michael E. DeBakey, M.D., Professorship in Pharmacology to J.W. and the seed funding for Center for NextGen Therapeutics.

References

(1) Park, J.; Cho, J.; Song, E. J. Ubiquitin-Proteasome System (UPS) as a Target for Anticancer Treatment. *Arch. Pharm. Res.* **2020**, *43* (11), 1144–1161. https://doi.org/10.1007/s12272-020-01281-8.

(2) Mullard, A. Targeted Protein Degraders Crowd into the Clinic. *Nat. Rev. Drug Discov.* **2021**, *20* (4), 247–250. https://doi.org/10.1038/d41573-021-00052-4.

(3) Fisher, S. L.; Phillips, A. J. Targeted Protein Degradation and the Enzymology of Degraders. *Curr. Opin. Chem. Biol.* **2018**, *44*, 47–55. https://doi.org/10.1016/j.cbpa.2018.05.004.

(4) Burslem, G. M.; Smith, B. E.; Lai, A. C.; Jaime-Figueroa, S.; McQuaid, D. C.; Bondeson, D. P.; Toure, M.; Dong, H.; Qian, Y.; Wang, J.; Crew, A. P.; Hines, J.; Crews, C. M. The Advantages of Targeted Protein Degradation Over Inhibition: An RTK Case Study. *Cell Chem. Biol.* **2018**, *25* (1), 67-77.e3. https://doi.org/10.1016/j.chembiol.2017.09.009.

(5) Békés, M.; Langley, D. R.; Crews, C. M. PROTAC Targeted Protein Degraders: The Past Is Prologue. *Nat. Rev. Drug Discov.* **2022**, *21* (3), 181–200. https://doi.org/10.1038/s41573-021-00371-6.

(6) Tsai, J. M.; Nowak, R. P.; Ebert, B. L.; Fischer, E. S. Targeted Protein Degradation: From Mechanisms to Clinic. *Nat. Rev. Mol. Cell Biol.* **2024**, *25* (9), 740–757. https://doi.org/10.1038/s41580-024-00729-9.

(7) Garber, K. The PROTAC Gold Rush. *Nat. Biotechnol.* **2021**. https://doi.org/10.1038/s41587-021-01173-2.

(8) Oleinikovas, V.; Gainza, P.; Ryckmans, T.; Fasching, B.; Thomä, N. H. From Thalidomide to Rational Molecular Glue Design for Targeted Protein Degradation. *Annu. Rev. Pharmacol. Toxicol.* **2024**, *64* (Volume 64, 2024), 291–312. https://doi.org/10.1146/annurev-pharmtox-022123-104147.

(9) Krönke, J.; Udeshi, N. D.; Narla, A.; Grauman, P.; Hurst, S. N.; McConkey, M.; Svinkina, T.; Heckl, D.; Comer, E.; Li, X.; Ciarlo, C.; Hartman, E.; Munshi, N.; Schenone, M.; Schreiber, S. L.; Carr, S. A.; Ebert, B. L. Lenalidomide Causes Selective Degradation of IKZF1 and IKZF3 in Multiple Myeloma Cells. *Science* **2014**, *343* (6168), 301–305. https://doi.org/10.1126/science.1244851.

(10) Petzold, G.; Fischer, E. S.; Thomä, N. H. Structural Basis of Lenalidomide-Induced CK1α Degradation by the CRL4(CRBN) Ubiquitin Ligase. *Nature* **2016**, *532* (7597), 127–130. https://doi.org/10.1038/nature16979.

(11) Watson, E. R.; Novick, S.; Matyskiela, M. E.; Chamberlain, P. P.; H de la Peña, A.; Zhu, J.; Tran, E.; Griffin, P. R.; Wertz, I. E.; Lander, G. C. Molecular Glue CELMoD Compounds Are Regulators of Cereblon Conformation. *Science* **2022**, *378* (6619), 549–553. https://doi.org/10.1126/science.add7574.

(12) Rankovic, Z.; Wu, Q.; Yang, J.; Nishiguchi, G.; Daub, H.; Shashikadze, B.; Machata, S.; Graef, T.; Schwalb, B.; Bartoschek, D.; Ohmayer, U.; Bednarz, A. H.; McGowan, K.; Shi, Z.; Price, J.; Mayasundari, A.; Yang, L.; Demichev, V.; Steger, M. Unbiased Mapping of Cereblon Neosubstrate Landscape by High-Throughput Proteomics. bioRxiv October 19, 2024, p 2024.10.18.618633. https://doi.org/10.1101/2024.10.18.618633.

(13) Cao, S.; Kang, S.; Mao, H.; Yao, J.; Gu, L.; Zheng, N. Defining Molecular Glues with a Dual-Nanobody Cannabidiol Sensor. *Nat. Commun.* **2022**, *13* (1), 815. https://doi.org/10.1038/s41467-022-28507-1.

(14) Hanzl, A.; Inghelram, C.; Schmitt, S.; Thomä, N. H. Primed for Degradation: How Weak Protein Interactions Enable Molecular Glue Degraders. *Curr. Opin. Struct. Biol.* **2025**, *92*, 103052. https://doi.org/10.1016/j.sbi.2025.103052.

(15) Ito, T.; Ando, H.; Suzuki, T.; Ogura, T.; Hotta, K.; Imamura, Y.; Yamaguchi, Y.; Handa, H. Identification of a Primary Target of Thalidomide Teratogenicity. *Science* **2010**, *327* (5971), 1345–1350. https://doi.org/10.1126/science.1177319.

(16) Lu, G.; Middleton, R. E.; Sun, H.; Naniong, M.; Ott, C. J.; Mitsiades, C. S.; Wong, K.-K.; Bradner, J. E.; Kaelin, W. G. The Myeloma Drug Lenalidomide Promotes the Cereblon-Dependent

Destruction of Ikaros Proteins. *Science* **2014**, *343* (6168), 305–309. https://doi.org/10.1126/science.1244917.
(17) Sievers, Q. L.; Petzold, G.; Bunker, R. D.; Renneville, A.; Słabicki, M.; Liddicoat, B. J.; Abdulrahman, W.; Mikkelsen, T.; Ebert, B. L.; Thomä, N. H. Defining the Human C2H2 Zinc Finger Degrome Targeted by Thalidomide Analogs through CRBN. *Science* **2018**, *362* (6414), eaat0572. https://doi.org/10.1126/science.aat0572.
(18) Baek, K.; Metivier, R. J.; Roy Burman, S. S.; Bushman, J. W.; Yoon, H.; Lumpkin, R. J.; Abeja, D. M.; Lakshminarayan, M.; Yue, H.; Ojeda, S.; Verano, A. L.; Gray, N. S.; Donovan, K. A.; Fischer, E. S. Unveiling the Hidden Interactome of CRBN Molecular Glues with Chemoproteomics. *BioRxiv Prepr. Serv. Biol.* **2024**, 2024.09.11.612438. https://doi.org/10.1101/2024.09.11.612438.
(19) Petzold, G.; Gainza, P.; Annunziato, S.; Lamberto, I.; Trenh, P.; McAllister, L. A.; DeMarco, B.; Schwander, L.; Bunker, R. D.; Zlotosch, M.; SriRamaratnam, R.; Gilberto, S.; Langousis, G.; Donckele, E. J.; Quan, C.; Strande, V.; Donatis, G. M. D.; Alabi, S. B.; Alers, J.; Matysik, M.; Staehly, C.; Dubois, A.; Osmont, A.; Garskovas, M.; Lyon, D.; Wiedmer, L.; Oleinikovas, V.; Lieberherr, R.; Rubin, N. T.; Lam, D. T.; Widlund, N. I.; Ritzen, A.; Caceres, R. M.; Vigil, D.; Tsai, J.; Wallace, O.; Peluso, M.; Sadok, A.; Paterson, A.; Zarayskiy, V.; Fasching, B.; Bonenfant, D.; Warmuth, M.; Castle, J.; Townson, S. A. Mining the CRBN Target Space Redefines Rules for Molecular Glue-Induced Neosubstrate Recognition. bioRxiv October 9, 2024, p 2024.10.07.616933. https://doi.org/10.1101/2024.10.07.616933.
(20) Dong, G.; Ding, Y.; He, S.; Sheng, C. Molecular Glues for Targeted Protein Degradation: From Serendipity to Rational Discovery. *J. Med. Chem.* **2021**, *64* (15), 10606–10620. https://doi.org/10.1021/acs.jmedchem.1c00895.
(21) Koduri, V.; Duplaquet, L.; Lampson, B. L.; Wang, A. C.; Sabet, A. H.; Ishoey, M.; Paulk, J.; Teng, M.; Harris, I. S.; Endress, J. E.; Liu, X.; Dasilva, E.; Paulo, J. A.; Briggs, K. J.; Doench, J. G.; Ott, C. J.; Zhang, T.; Donovan, K. A.; Fischer, E. S.; Gygi, S. P.; Gray, N. S.; Bradner, J.; Medin, J. A.; Buhrlage, S. J.; Oser, M. G.; Kaelin, W. G. Targeting Oncoproteins with a Positive Selection Assay for Protein Degraders. *Sci. Adv.* **2021**, *7* (6), eabd6263. https://doi.org/10.1126/sciadv.abd6263.
(22) Mayor-Ruiz, C.; Bauer, S.; Brand, M.; Kozicka, Z.; Siklos, M.; Imrichova, H.; Kaltheuner, I. H.; Hahn, E.; Seiler, K.; Koren, A.; Petzold, G.; Fellner, M.; Bock, C.; Müller, A. C.; Zuber, J.; Geyer, M.; Thomä, N. H.; Kubicek, S.; Winter, G. E. Rational Discovery of Molecular Glue Degraders via Scalable Chemical Profiling. *Nat. Chem. Biol.* **2020**, *16* (11), 1199–1207. https://doi.org/10.1038/s41589-020-0594-x.
(23) Yamanaka, S.; Horiuchi, Y.; Matsuoka, S.; Kido, K.; Nishino, K.; Maeno, M.; Shibata, N.; Kosako, H.; Sawasaki, T. A Proximity Biotinylation-Based Approach to Identify Protein-E3 Ligase Interactions Induced by PROTACs and Molecular Glues. *Nat. Commun.* **2022**, *13* (1), 183. https://doi.org/10.1038/s41467-021-27818-z.
(24) Costacurta, M.; Sandow, J. J.; Maher, B.; Susanto, O.; Vervoort, S. J.; Devlin, J. R.; Garama, D.; Condina, M. R.; Steele, J. R.; Kahrood, H. V.; Gough, D.; Johnstone, R. W.; Shortt, J. Mapping the IMiD-Dependent Cereblon Interactome Using BioID-Proximity Labelling. *FEBS J.* **2024**, *291* (22), 4892–4912. https://doi.org/10.1111/febs.17196.
(25) Che, X.; Team, T. S. M. I. YDS-GlueFold: Surpassing AlphaFold 3-Type Models for Molecular Glue-Induced Ternary Complex Prediction. bioRxiv April 16, 2025, p 2024.12.23.630090. https://doi.org/10.1101/2024.12.23.630090.
(26) Dudas, B.; Athanasiou, C.; Mobarec, J. C.; Rosta, E. Quantifying Cooperativity through Binding Free Energies in Molecular Glue Degraders. *J. Chem. Theory Comput.* **2025**. https://doi.org/10.1021/acs.jctc.5c00064.
(27) Shalom, B.; Salaymeh, Y.; Risling, M.; Katzav, S. Unraveling the Oncogenic Potential of VAV1 in Human Cancer: Lessons from Mouse Models. *Cells* **2023**, *12* (9), 1276. https://doi.org/10.3390/cells12091276.

(28) Ksionda, O.; Saveliev, A.; Köchl, R.; Rapley, J.; Faroudi, M.; Smith-Garvin, J. E.; Wülfing, C.; Rittinger, K.; Carter, T.; Tybulewicz, V. L. J. Mechanism and Function of Vav1 Localisation in TCR Signalling. *J. Cell Sci.* **2012**, *125* (22), 5302–5314. https://doi.org/10.1242/jcs.105148.
(29) Neurath, M. F.; Berg, L. J. VAV1 as a Putative Therapeutic Target in Autoimmune and Chronic Inflammatory Diseases. *Trends Immunol.* **2024**, *45* (8), 580–596. https://doi.org/10.1016/j.it.2024.06.004.
(30) Razidlo, G. L.; Magnine, C.; Sletten, A. C.; Hurley, R. M.; Almada, L. L.; Fernandez-Zapico, M. E.; Ji, B.; McNiven, M. A. Targeting Pancreatic Cancer Metastasis by Inhibition of Vav1, a Driver of Tumor Cell Invasion. *Cancer Res.* **2015**, *75* (14), 2907–2915. https://doi.org/10.1158/0008-5472.CAN-14-3103.
(31) Lin, H.; Riching, K.; Lai, M. P.; Lu, D.; Cheng, R.; Qi, X.; Wang, J. Lysineless HiBiT and NanoLuc Tagging Systems as Alternative Tools for Monitoring Targeted Protein Degradation. *ACS Med. Chem. Lett.* **2024**, *15* (8), 1367–1375. https://doi.org/10.1021/acsmedchemlett.4c00271.
(32) Min, J.; Mayasundari, A.; Keramatnia, F.; Jonchere, B.; Yang, S. W.; Jarusiewicz, J.; Actis, M.; Das, S.; Young, B.; Slavish, J.; Yang, L.; Li, Y.; Fu, X.; Garrett, S. H.; Yun, M.-K.; Li, Z.; Nithianantham, S.; Chai, S.; Chen, T.; Shelat, A.; Lee, R. E.; Nishiguchi, G.; White, S. W.; Roussel, M. F.; Potts, P. R.; Fischer, M.; Rankovic, Z. Phenyl-Glutarimides: Alternative Cereblon Binders for the Design of PROTACs. *Angew. Chem. Int. Ed.* **2021**, *60* (51), 26663–26670. https://doi.org/10.1002/anie.202108848.
(33) Norris, S.; Ba, X.; Rhodes, J.; Huang, D.; Khambatta, G.; Buenviaje, J.; Nayak, S.; Meiring, J.; Reiss, S.; Xu, S.; Shi, L.; Whitefield, B.; Alexander, M.; Horn, E. J.; Correa, M.; Tehrani, L.; Hansen, J. D.; Papa, P.; Mortensen, D. S. Design and Synthesis of Novel Cereblon Binders for Use in Targeted Protein Degradation. *J. Med. Chem.* **2023**, *66* (23), 16388–16409. https://doi.org/10.1021/acs.jmedchem.3c01848.